Asian Journal of Chemistry Vol. 22, No. 9 (2010), 7410-7422

Preparation, Characterization of (SBA-15)-TiO_2 Nanocomposite Material and Its Application to Wiping Off Methylene Blue in Water Body

YU-QIN MA†, HUI YU‡, RAO MENG†, XIN JIN†, QING-ZHOU ZHAI‡ and JING-BO XU*
School of Urban and Environmental Sciences,
Northeast Normal University, Changchun 130024, P.R. China
Fax: (86)(431)85383815; Tel: (88)(431)85319393; E-mail:xujb515@nenu.edu.cn

Titania (TiO_2) was incorporated into SBA-15 by solid phase thermal diffusion method and the prepared nanocomposite material was characterized by powder X-ray diffraction, Fourier transform infrared spectroscopy, nitrogen adsorption-desorption analysis, transmission electron microscopy and scanning electron microscopy. The results showed that for the (SBA-15)-TiO_2 the frameworks and ordered mesoporous structures of the SBA-15 molecular sieve were kept well. When the (SBA-15)-TiO_2 was used to remove the methylene blue in water body, the removal effect was good.

Key Words: Methylene blue, Photocatalysis, Titania, SBA-15.

INTRODUCTION

Since the photo-redox of titania was first discovered, internal and overseas researchers have done a lot of researches on its photocatalytic mechanism and on improving its catalytic efficiency. The studies show that photo-redox of titania is caused by the holes and electrons which are produced by the function of photons excitation. The holes or electrons react to the substance which is absorbed on the surface of titania. Meanwhile, the electrons go along composite with the holes and competed with redox. Therefore, the major methods to improve catalytic efficiency of the titania are increasing the degree of the separation of hole-electron pairs and adjusting absorption characteristics of the surface of catalyst. For the anterior, we can introduce defect into catalyst to enhance the capture of electron and to increase the amount of isolated hole. For example, anatase type titania with more defect has higher photo-catalytic activity compared to rutile type. Besides, appropriate size decreasing of catalyst particles contributes to the separation of hole-electron. However,

†School of Chemistry and Environmental Engineering, Changchun University of Science and Technology, Changchun 130022, P.R. China.
‡Research Center for Nanotechnology, Changchun University of Science and Technology, Changchun 130022, P.R. China.

too smaller size may increase the probability of composition of hole-electron pairs and enhance the rate of composition[1]. Biswas and Almquist[2] found that titania of 16 nm had the highest catalytic efficiency when they studied the photo-oxidation of cyclohexane on titanium dioxide. The catalytic efficiency decreased when the size of the catalyst particles decrease. To adjusting absorption characteristics of the surface of catalyst, the methods like changing hydrophilic or lipophilic property of the surface, decreasing the size of particles, increasing surface, *etc*. can be used. Nano-titania is an environmentally friendly catalyst with high photo-catalytic activity. In order to enhance its properties, people control the size in nanoscale to raise its photo-catalytic activity during photo-catalytic reaction. However, nano-material may aggregate and be difficult to be recycled[3] when it is too small.

Photo-catalytic degradation of titania has been a hot-spot in sewage treatment in recent years and been paid attention by researchers as it can degrade contaminants completely and economically. The photo-catalytical treatment of waste water has numerous advantages: (1) It has the wide range of action and effective to the most deoxidizing contaminants in water. (2) Thorough oxidation, no accumulation of intermediate products, no secondary pollution, degrading chlorinated phenols organic into CO_2 and Cl^-. (3) High translation ratio and reaction rapidity and low cost[4,5].

Mesoporous material refers to material with ordered pore of 2-50 nm. But the mesoporous pore is formed by amorphous pore wall, so mesoporous material has lower thermal stability and hydrothermal stability compared to microporous zeolite[6]. At the end of 20th century, Zhao *et al.*[7] introduced triblock copolymer as template to synthesize SBA-15 mesoporous molecular sieve and enhanced its thermal stability and hydrothermal stability to some extent. The SBA-15 has large pore diameter, high specific surface area and hydrothermal stability. It is promising in the application of catalysis, bio-separation, molecular assembly and chromatographic carrier.

The immobility of titania into the pores of porous SiO_2 material not only makes for distribution and recycle use of titania particulates, but also controls the size of nano-particulates through the pores of mesoporous materials. At the same time, because titania is transparent to UV-vis light and the loaded nanoscale titania particulates are not highly effected by light intensity, photo-catalysis activity are not decreased by loading. It becomes a hot-spot[8]. Wang *et al.*[3] used titanium isopropoxide to hydrolyze in the pores of SBA-15 using isopropyl alcohol as a medium and obtained material containing 24.4 % TiO_2. They controlled the size of TiO_2 particulates and increased the content of TiO_2 by multi-step impregnation method. The obtained material was used to photo-degradation of estrogens and phenol and the reactive activity was higher. Busuioc *et al.*[9] used titanium isopropoxide as source of titanium to be hydrolyzed in acidic solution and obtained nano-TiO_2. Then, it was used in the degradation of rhodamine-6G and the relation between absorption and photo-degradation was analyzed. Jung *et al.*[10] brought a

small amount of Ti into the frameworks of SBA-15 by one-step hydrothermal synthesis, then incorporated Ti more by impregnating in the pores of SBA-15 and calcined to obtain photo-catalyst. Then, the catalytic activity was inspected by using the UV light degradation of orange yellow II as probes.

This study incorporated TiO_2 into the pores of SBA-15 molecular sieve by solid phase thermal diffusion method. A series of techniques such as X-ray powder diffraction (XRD) were used to characterize the structure of the material. Research showed that the (SBA-15)-TiO_2 kept the ordered mesoporous pore structure and TiO_2 mainly distributed in the mesoporous of SBA-15 molecular sieve. The organic contaminants in water are harmful to the environment and human body. Some of them are difficult to be degraded under natural conditions or by microbial ways. Methylene blue is an organic dye and is one of the organic contaminants in waste water of printing and dyeing. It is hardly naturally degraded. In this article the (SBA-15)-TiO_2 composite material was used as catalyst in photo-degradation of methylene blue and its catalytic conditions of the catalyst were optimized. Through comparison of catalysis, we discovered that methylene blue could be degraded completely within 10 min under the catalysis of (SBA-15)-TiO_2, while there was still a lot of methylene blue that was not degraded after 60 min under the catalysis of regular nano-TiO_2. Thus, the (SBA-15)-TiO_2 prepared in the present study has an excellent photo-catalytic degradation effect on methylene blue.

EXPERIMENTAL

Tetraethyl orthosilicate (TEOS, A.R., Shanghai Chemical Pharmaceutical Co., Ltd. China), biparental triblock copolymer, poly(1,2-ethylene glycol)-block-poly (propylene glycol)-block-poly(1,2-ethylene glycol) (Fluka, Switzerland), nano-TiO_2 powder (anatase type, 20 nm, Degusa Germany), methylene blue (Sinopharm Chemical Reagent Co., Ltd). All the reagents used in the experiment were of analytical grade, all water was deionized water.

Preparation of SBA-15 mesoporous molecular sieve: The hydrothermal synthesis method was used to prepare SBA-15 mesoporous molecular sieve in the experiment[7]. The SBA-15 molecular sieve was synthesized using tetraethyl orthosilicate (TEOS) as silica resource, using triblock copolymers ($EG_{20}PG_{40}EG_{20}$) as template, in acidic medium. At first, 2 g of biparental triblock copolymers was dissolved in 15 g of deionized water and 60 g of 2 mol L^{-1} hydrochloric acid solution and stirred. After forming a homogeneous solution, 4.25 g of TEOS was slowly added into the solution. The mixed solution was stirred for 24 h at 40 ºC. The mixed solution was put into the reaction vessel with plastic substrates at 100 ºC for 2 days. The product was filtered and washed with deionized water and dried at room temperature. The material was calcined at temperature 550 ºC for 24 h to completely eliminate the template. Then, the white powder of SBA-15 molecular sieve was gained.

Solid-phase thermal diffusion method loaded TiO_2 into the channels of SBA-15 molecular sieve: 1.0 g of the SBA-15 was mixed with 0.20 g of the nano-TiO_2, homogeneously. The mixture was calcined at 500 ºC for 48 h. Then, the product was cooled down to room temperature in oven and a white powder was obtained. The sample was designed as (SBA-15)-TiO_2.

Photocatalytic degradation of methylene blue with (SBA-15)-TiO_2: The material (SBA-15)-TiO_2 was immersed into the certain concentration solutions of methylene blue, stirred at room temperature. A 300 W high-pressure mercury lamp was used as the light source and for the mixed solution, reaction went under the irradiation. The sample was collected at regular intervals. The transparent liquid was segregated from the mixture by high centrifugation. The upper clear solution was taken and the remaining methylene blue was analyzed by UV-Vis spectroscopy.

Characterization of catalysts: Small-angle powder X-ray diffraction (XRD) patterns were collected on a D5005 diffractometer (Siemens, Germany) with Cu-K_α radiation (λ = 1.5418 Å and operated at 30 kV and 20 mA). Fourier transform infrared (FT-IR) spectra were recorded on a Bruker Vertex-70 FT-IR spectrophotometer using a KBr pellet technique to characterize the framework of the sample (The typical pellet consists of 1 wt% sample and 99 wt% KBr). Physical adsorption of nitrogen was performed on a Micromeritics ASAP2010M volumetric adsorption analyzer at 77 K. The framework structure (pore size, pore volume and the surface area) of the sample was mensurated. A sample was degassed in vacuum at 573 K for 12 h before measurement. The specific surface area measurement was performed according to the BET (Brunner-Emmett-Teller) method[11]. Pore size distribtion was obtained by applying the BJH (Barrett-Joyner-Halenda) model[12]. Transmission electron microscopy (TEM) images were taken on a JEOL 2010 TEM instrument. Scanning electron microscopy (SEM) photograph was determined on a JEOL JSM-5600L SEM instrument. The content of methylene blue in the sample was measured on a UV-2550 UV-VIS spectrophotometer (Shimadzu, Japan) and the wavelength range was in the range of 200-1200 nm.

RESULTS AND DISCUSSION

Powder X-ray diffraction analysis (XRD): Fig. 1 shows the small-angle XRD patterns of the SBA-15 and the (SBA-15)-TiO_2 host-guest composite material. From Fig. 1, it can be seen that the curves of the prepared samples show three diffraction peaks denoted as (100), (110) and (200), respectively, which are consistent with the diffraction peaks of the SBA-15 molecular sieve reported in the reference[7]. It shows that the well-ordered hexagonal mesoporous arrays with 2-dimensional channels were maintained in the (SBA-15)-TiO_2 sample.

Fig. 2 shows the wide-angle XRD patterns of the SBA-15, nano-TiO_2 and the (SBA-15)-TiO_2 host-guest nanocomposite material. The diffraction peaks of TiO_2 appeared for the (SBA-15)-TiO_2 sample. It can be explained that the content of TiO_2 is relatively high. The partial TiO_2 exists in the form of crystal in the molecular sieve.

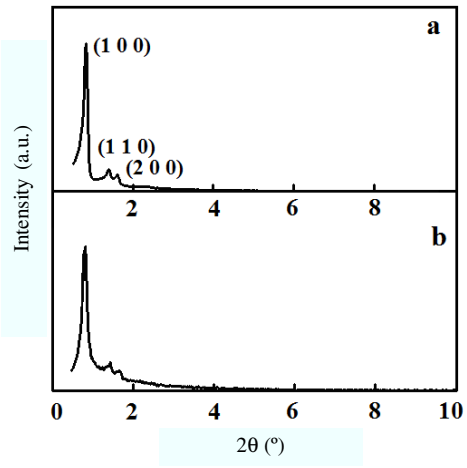

Fig. 1. Small-angle XRD patterns of the samples a) SBA-15, b)(SBA-15)-TiO_2

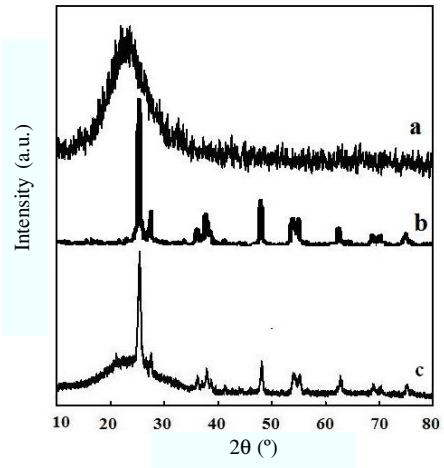

Fig. 2. Wide-angle XRD patterns of the samples a) SBA-15, b) nano-TiO_2, c) (SBA-15)-TiO_2

Fourier transform infrared (FT-IR) spectra: Fig. 3 shows the FT-IR spectra of the (SBA-15)-TiO_2 composite materials, SBA-15 molecular sieve and nano-TiO_2. From the FT-IR analysis, it is found that there is no structural collapse of pore structures occurred by the incorporation of TiO_2. This shows that the destructive actions of the TiO_2 guest material and its middle products were very small.

In the IR pattern (Fig. 3), each sample has four peaks for (SBA-15)-TiO_2 sample and the SBA-15 molecular sieve. The bands that locate at 463 cm^{-1} for the sample SBA-15 molecular sieve and at 467 cm^{-1} for the (SBA-15)-TiO_2 sample correspond to T-O bending. The bands that locate at 802 cm^{-1} for the SBA-15 molecular sieve sample and at 803 cm^{-1} for the (SBA-15)-TiO_2 sample can be assigned to TO_4 symmetric stretching of Si-O-Si. The bands at 1084 cm^{-1} for the SBA-15 molecular sieve sample and at 1083 cm^{-1} for the (SBA-15)-TiO_2 sample can be assigned to TO_4 asymmetric stretching of Si-O-Si[13]. The band that locates at 959 cm^{-1} is corresponding to the stretching of nonbridging oxygen atoms of Si-OH.

In the IR pattern (Fig. 3), nano-TiO_2 sample has two peaks which locate at 657 and 1103 cm^{-1}. The sample (SBA-15)-TiO_2 shows a band locating at 655 cm^{-1}, which is corresponding to that of TiO_2. It might be interpreted that the TiO_2 component has been doped in the pores, or equally dispersed on the surface of SBA-15. At the same time, the band that locates at 959 cm^{-1} corresponding to the stretching of nonbridging oxygen atoms of Si-OH disappeared in the IR pattern of the (SBA-15)-TiO_2. It might be interpreted that the guest TiO_2 component substituted the -OH of Si-OH.

Low temperature nitrogen adsorption-desorption isotherms: Fig. 4 shows the low temperature nitrogen adsorption-desorption isotherms of the SBA-15 and (SBA-15)-TiO_2. From the isotherms, the low temperature nitrogen adsorption-desorption isotherm of (SBA-15)-TiO_2 is similar to that of the SBA-15, showing

typical irreversible type IV adsorption isotherms with a H1 hysteresis loop which are characteristic of mesoporous materials with 1-D cylindrical channels as defined by IUPAC[14]. There are clear adsorption and desorption branches on the nitrogen adsorption-desorption isotherms of the samples. The isotherms of the samples featured hysteresis loops with sharp adsorption and desorption branches. The sharpness of the adsorption branches is indicative of a narrow mesopore size distribution (Fig. 5).

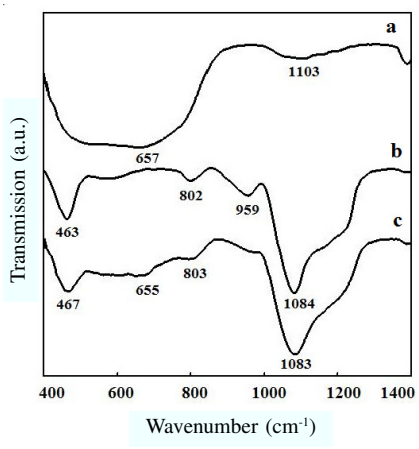

Fig. 3. Infrared spectra of each sample: a) TiO_2, b) SBA-15, c) (SBA-15)-TiO_2

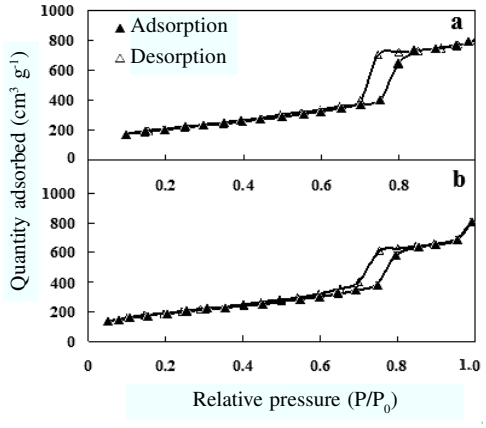

Fig. 4. Low temperature nitrogen adsorption-desorption isotherms of sample. (▲ desorption; △ adsorption) a) SBA-15, b) (SBA-15)- TiO_2

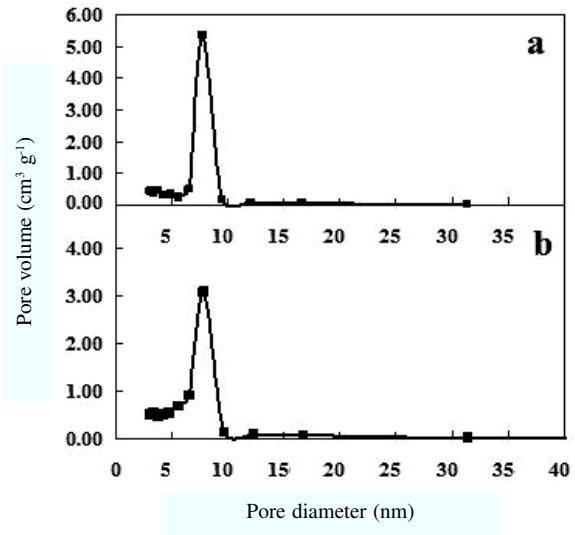

Fig. 5. Pore size distribution patterns of the samples: a) SBA-15, b) (SBA-15)-TiO_2

At the relatively low pressure, the adsorption of the materials is mainly monolayer adsorption. Under the situation, the narrow pore structure does not block the adsorption of gas from pore-blocking and the capillary condensation can not occur. Adsorption and desorption process are reversible. After that, with the rise of the relatively pressure and the increase of the adsorbed gas volume in pore gradually, the adsorption mainly is multilayer adsorption. The adsorbed gas volume adds rapidly. To the SBA-15, for both adsorption and desorption branches one jump appears when relative pressures (p/p_0) reached 0.75. To the (SBA -15)-TiO_2, the foregoing phenomenon occurred when the p/p_0 reached 0.65. It can be explained that the relative pressure increased to the degree that capillary condensation occurred.

There are clear hysteresis loops on nitrogen adsorption-desorption isotherms. The appearance shows that adsorption and desorption processes are irreversible. It attributes to the contraction of cylindrical pores which delay capillary evaporation process[15,16]. Thus, adsorption and desorption processes can occur in different relatively pressure. In the material having mesopores, for the capillary condensation the relative pressure is an increasing function of the pore diameter. The pore diameter is larger and the relative partial pressure of the capillary condensation phenomenon becomes higher (Fig. 5 and Table-1). Furthermore, the delayed action appeared under the relatively higher pressure which corresponds to the mesoporosity character of the SBA-15. This demonstrates that the mesoporous pores still existed and have not been destroyed after the TiO_2 was assembled into the pores of the SBA-15.

TABLE-1
PORE STRUCTURE PARAMETERS OF SAMPLES

Sample	d_{100} (nm)	a_0* (nm)	Specific surface area (m^2/g)	Pore volume** (cm^3/g)	Pore size*** (nm)
SBA-15	10.50	12.12	662.2	1.267	7.67
(SBA-15)- TiO_2	10.76	12.42	586.7	1.136	6.87

*$a_0 = \frac{2}{\sqrt{3}} d_{100}$; **BJH desorption cumulative volume of pores;

***Pore size calculated from the desorption branch.

When the relative pressure reached 0.85 for the SBA-15 and 0.86 for (SBA-15)-TiO_2 nanocomposite material, the adsorption and desorption branches in the isotherm lap over again. This is because the pores have been permeated by the adsorptive gas and the capillary condensation has been finished. The adsorption process and desorption process mainly carry out on the outer surface of the molecular sieve and this process is reversible.

The specific surface areas of the SBA-15 and (SBA-15)-TiO_2 were calculated by BET method[11]. The pore size distribution was calculated by using the Barrett, Joyner and Halenda (BJH) equation[12]. The parameters were calculated from the desorption branch of nitrogen adsorption-desorption isotherms. Compared with

SBA-15, the BET specific surface area, the pore diameter and the pore volume of (SBA-15)-TiO_2 were all decreased because of the incorporation of the TiO_2 (Table-1). It can be concluded that the TiO_2 guest material has been assembled into the pores of the SBA-15.

Transmission electron microscopy (TEM): Fig. 6 shows the TEM images of the samples. All micrographs are recorded with the electron beam direction parallel to and perpendicular to the channel direction. TEM experiments (Fig. 6) show that the (SBA-15)-TiO_2 sample has the well-ordered hexagonal arrays of mesopores from the images viewed perpendicular to the pore axis. The straight lattice fringes are seen from the images viewed along to the pore axis. From the TEM images, the (SBA-15)-TiO_2 sample has a 2-D hexagonal structure of a p6mm symmetry. The TEM images in Fig. 6 show that the highly ordered mesoporous structure of SBA-15 is remained after the formation of TiO_2 inside the SBA-15 channels.

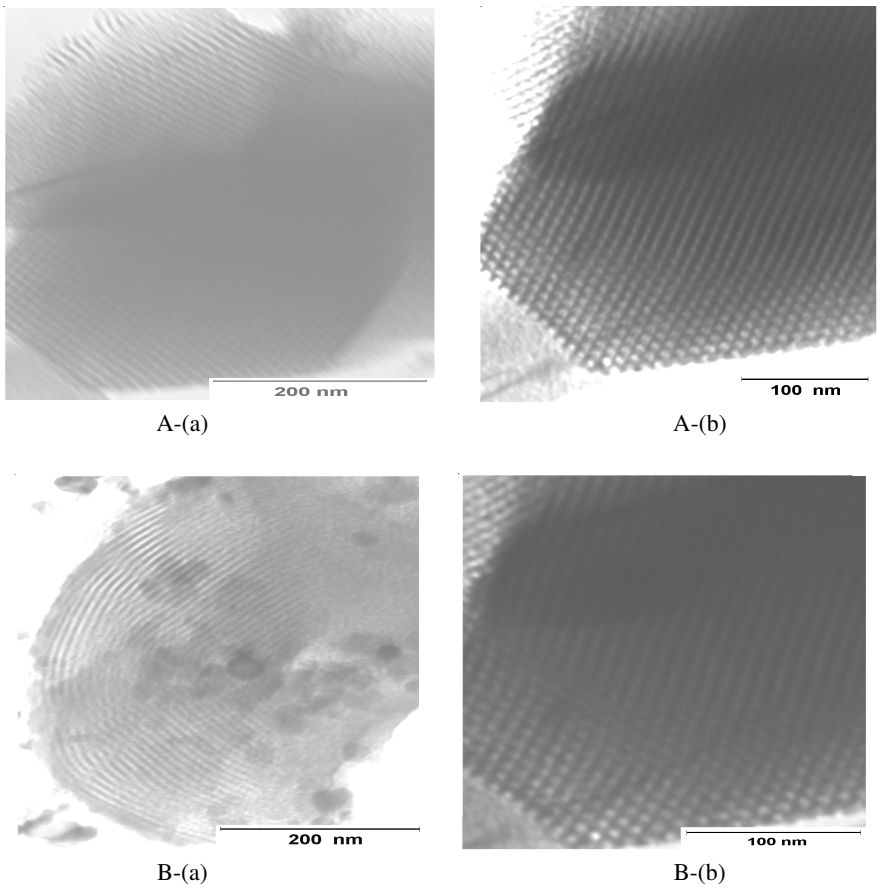

A-(a) A-(b)

B-(a) B-(b)

Fig. 6. TEM image of the samples (A) SBA-15, (B) (SBA-15)-TiO_2: (a) taken with the beam direction parallel to the pores b) taken with the beam direction perpendicular to the pores

Scanning electron microscopy (SEM): The SEM analyses of the samples (Fig. 7) show that the primary particles of the samples present fibriform particle. From account, the particle diameters of the samples are as follows: the SBA-15 molecular sieve particle diameter is 333 ± 10 nm and the (SBA-15)-TiO_2 sample particle diameter is 340 ± 10 nm. From the results of the SEM analyses, the SBA-15 particle diameter has a smaller increase after the formation of TiO_2 inside the SBA-15 channels. However, the fibriform particle of the prepared samples is remained.

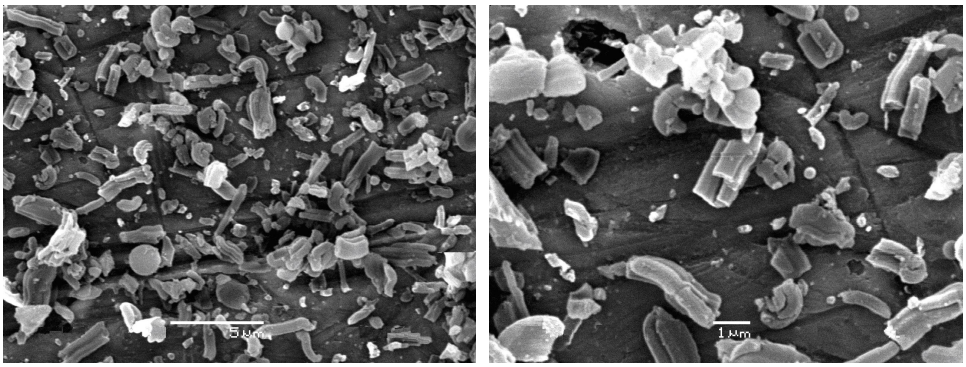

(a) (b)

Fig. 7. SEM image of the samples: (a) SBA-15, (b) (SBA-15)- TiO_2

Photo-catalytic effect: Fig. 8 shows the UV-Vis diffuse reflection absorption spectra of methylene blue and nano-TiO_2. The UV-Vis diffuse reflection absorption spectrum of methylene blue has narrow characteristic absorption peaks at 664, 291 and 246 nm, respectively. The UV-Vis diffuse reflection absorption spectrum of nano-TiO_2 has a wide characteristic absorption peak at 283 nm.

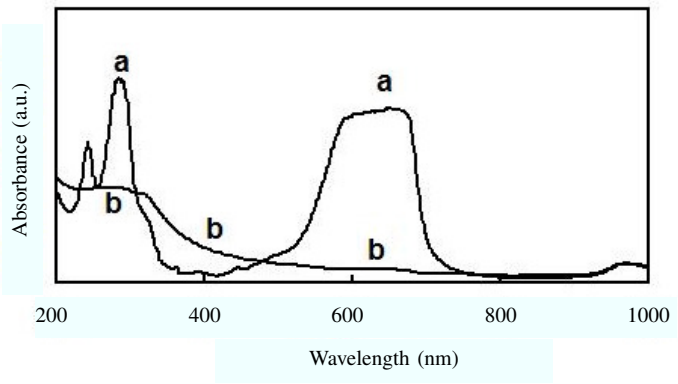

Fig. 8. UV-Vis diffuse reflection absorption spectra of the samples: (a) methylene blue, (b) nano-TiO_2

Influence of solution pH value on photo-catalytic activity: 0.010 g of (SBA-15)-TiO_2 catalyst was added in 30 mL of 20 mg L^{-1} methylene blue solution. The pH values of the solution were adjusted by hydrochloric acid to 2.3, 5.2, 8.2, 10.2 and 12, respectively. The reactions were progressed under 300 W mercury lamp for 1 h. Then, the UV-visible absorption spectra of the methylene blue solution were determined and the results are shown as Fig. 9.

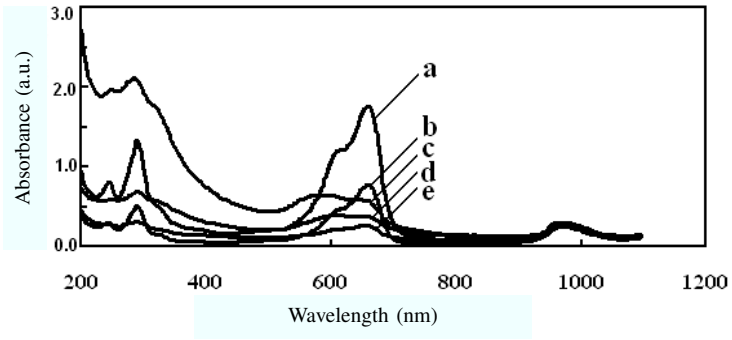

Fig. 9. UV-Vis diffuse reflection absorption spectra of the solution of degradation methylene blue at different pH value (a) pH = 2.3, (b) pH = 5.2, (c) pH = 12, (d) pH = 10.2, (e) pH = 8.2

From Fig. 9, it is clear that the pH value of the solution has a great effect on the (SBA-15)-TiO_2 photo-catalytic degradation to methylene blue. When the pH value of solution is smaller, the (SBA-15)-TiO_2 has almost no catalytic effect on the degradation of the methylene blue. The catalytic effect markedly increases with the increase of the pH. However, when the pH of the solution is too high, the catalytic effect begins to decrease with the increase of the pH. The titanium dioxide has the effect of degradation on organic matter. When the semiconductor of TiO_2 is excited by an UV irradiation with the wavelength of less than 400 nm, photoelectron (e^-) and holes (h^+) are produced:

$$TiO_2 + h\nu\ (\geq 3.2\ eV) \rightarrow e^- + h^+ \quad (1)$$

$$O_2\ (g) + e^- \rightarrow {}^{\bullet}O_2^- + H^+ \rightarrow {}^{\bullet}O_2H \quad (2)$$

$$h^+ + OH^- \rightarrow {}^{\bullet}OH \quad (3)$$

The photoelectron can be captured by the dissolved O_2 to generate the ${}^{\bullet}O_2^-$ which has a strong oxidizing power. The holes can be captured by the OH^- to generate ${}^{\bullet}OH$[17-19]. The lively free radicals can oxidize the methylene blue and the products are CO_2 and H_2O. According to the theory, in strong acidic or strong alkaline environment, the ionization degree of H_2O decreases which inhibits the reaction (2) or (3). Thus, the catalytic activity of the material (SBA-15)-TiO_2 is reduced.

Effects of two kinds of catalyst at different reaction time: According to the experimental method, 0.080 g of (SBA-15)-TiO_2 catalyst was acceded in 60 mL of 20 mg L^{-1} methylene blue solution. 0.016 g of pure nano-TiO_2 was acceded in 60

mL of 20 mg L^{-1} methylene blue solution in another reactor. Under centrifugal condition, the reactions were maintained for 10, 30, 50, 60 min, respectively. The results are shown in Fig. 10 and 11.

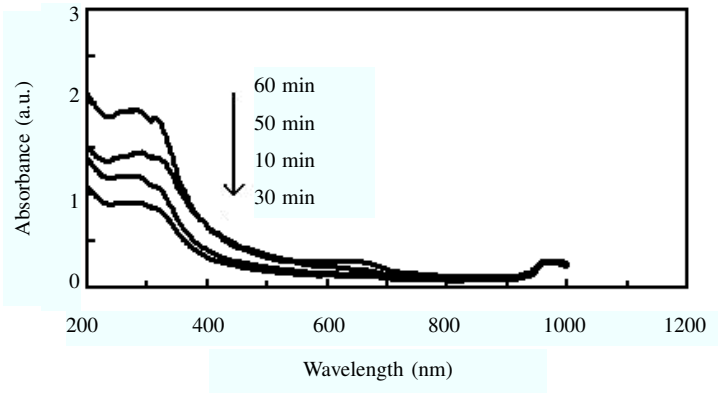

Fig. 10. UV-Vis diffuse reflection absorption spectra of the solution of degradation methylene blue at different time [(SBA-15)-TiO_2 was used as catalyzer]

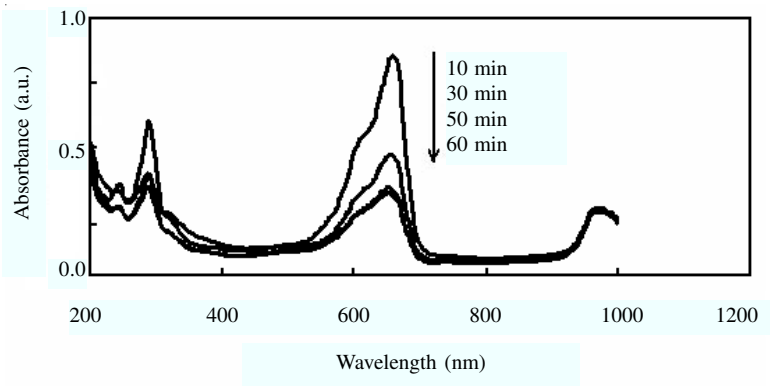

Fig. 11. UV-Vis diffuse reflection absorption spectra of the solution of degradation methylene blue at different time (nano-TiO_2 was used as catalyzer)

From Fig.10, the characteristic absorption peak of methylene blue has disappeared completely after 10 min. The only characteristic absorption peak of (SBA-15)-TiO_2 appeared at this time (as shown in Fig. 8 b). It shows that the methylene blue has been reacted completely.

Fig. 11 shows the UV-Vis diffuse reflection absorption spectra of degradation reaction of the methylene blue where pure nano-TiO_2 was used as catalyst. From Fig. 11, the intensity of absorption peak of the methylene blue falls gradually with the prolongation of the reaction time. However, there is still the strong absorption peak of methylene blue after 1 h. This shows that there is much methylene blue in the solution.

Fig. 12 shows the UV-Vis absorption spectra of the methylene blue which the SBA-15 molecular sieve is used as absorbent under no light irradiation conditions. From the spectra, the change of absorption peak intensity of the methylene blue is not large in the first 10 min. With reaction time extension, the absorption peak intensity of the methylene blue reduces gradually. The absorption peak appearance of the methylene blue is still strong after 1 h. It shows that there is still much of the methylene blue in the solution.

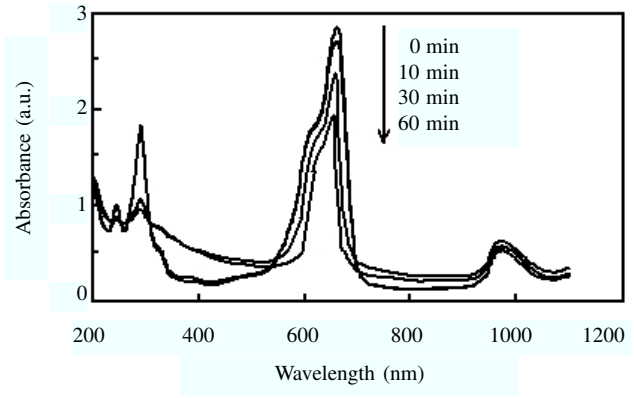

Fig. 12. UV-Vis diffuse reflection absorption spectra of the solution of degradation methylene blue at different time (SBA-15 was used as adsorbent)

Compared with the Figs. 10 and 11, the photo-catalytic speed of methylene blue is much faster than the nano-TiO_2 when the (SBA-15)-TiO_2 was used as catalyst. It is because that the catalyzer of the (SBA-15)-TiO_2 has enormous specific surface area, which can provide the more effective area for the photo-catalysis. The interfacial density increases when the organic material absorbs to the surface of the TiO_2. It is favorable to the degradation of the organic pollutants and the separation of semi-conductor photoelectron-hole. It accelerates the rate of the reaction and improves the catalytic efficiency.

Comparing Figs. 10 and 12, the adsorption behaviour of methylene blue is a very slow process in the SBA-15 molecular sieve. Its concentration change is less in initial 10 min. However, the methylene blue has been completely disappeared after 10 min under the function of the catalyst prepared in the present study. It can show that in 10 min the decisive action to the abstraction of methylene blue is the degradation function of the catalyst prepared in this study.

Conclusion

The following conclusions can be drawn from this study:

(1) TiO_2 can be incorporated into the (SBA-15) molecular sieve channels by thermal diffusion method. It has the advantages of the uniform distribution, high loading amount, *etc*.

(2) The (SBA-15)-TiO_2 host-guest nanocomposite material still has the characteristics of mesoporous material. The framework structure and the mesoporous channels of the SBA-15 molecular sieve are retained in the (SBA-15)-TiO_2 sample.

(3) The (SBA-15)-TiO_2 nanocomposite material which was prepared in this study has very high photo-catalytic degradation effect on methylene blue. Methylene blue is completely degraded in 10 min under the function of the (SBA-15)-TiO_2 catalyst, but it has not been completed after 1 h under the function of the conventional nano-TiO_2. It showed that the catalytic efficiency of the (SBA-15)-TiO_2 catalyst prepared in the present study is much better than that of the conventional nano-TiO_2.

ACKNOWLEDGEMENT

The authors are grateful to the financial support from Jilin Provincial Science and Technology Department. The grant number was 20090548 (KYC-JC-XM-2009-040).

REFERENCES

1. H.A. Xi, N.H. Fang, Z.K. Li, Y.B. Zhang, Q.H. Lu, J. Yin and Z.K. Zhu, *Acta Chim. Sinica*, **60**, 2124 (2002).
2. C.B. Almquist and P. Biswas, *Appl. Catal. A: General*, **214**, 259 (2001).
3. W. Wang and M .Song, *Mater. Res. Bull.*, **41**, 436 (2006).
4 J.Q. Wan, Y.W. Ma and Y. Zhang, *Trans. Chin. Pulp. Paper*, **19**, 62 (2004).
5. H.L. Lin, G.W. Zhou, Y. Liu, Z.Y. Shao and Q.H. Meng, *Nanosci. Nanotech.*, **3**, 27 (2006).
6. R.R. Xu and W.Q. Pang, Molecular Sieve and Porous Material Chemistry, Sci. Publish. House, Beijing, pp. 145–151 (2004).
7. D.Y. Zhao, J.L. Feng, Q.S. Huo, N. Melosh, G.H. Fredrickson, B.F. Chmelka and G.D. Stucky, *Science*, **279**, 548 (1998).
8. J.X. Su, W. Qu, L.Y. Ma, J. Yin and Q. Pan, *Acta Chim. Sinica*, **66**, 2416 (2008).
9. A.M. Busuioc, V. Meynen and E. Beyers, *Catal. Commun.*, **8**, 527 (2007).
10. W.Y. Jung, S.H. Baek and J.S. Yang, *Catal. Today*, **131**, 437 (2008).
11. S. Brunauer, P.H. Emmett and E. Teller, *J. Am. Chem. Soc.*, **60**, 309 (1938).
12. E.P. Barrett, L.G. Joyner and P.P. Halenda, *J. Am. Chem. Soc.*, **73**, 373 (1951).
13. S.Y. Yu, L.P. Wang and B. Chen, *Chem. Eur. J.*, **11**, 3894 (2005).
14. K.S.W. Sing, D.H. Everett, R.A.W. Haul, L. Moscow, R.A. Pierotti, T. Rouquerol and T. Siemienewska, *Pure. Appl. Chem.*, **57**, 603 (1985).
15. T.W. Kim, R. Ryong and K. Michal, *J. Phys. Chem. B*, **108**, 11480 (2004).
16. M. Kruk and M. Jaroniec, *J. Phys. Chem. B*, **106**, 4732 (2002).
17. R.W. Matthews and S.R. McEvoy, *J. Photochem. Photobiol. A*, **66**, 355 (1992).
18. S. Malato, J. Blanco, C. Richter, B. Braun and M.I. Maldonado, *Appl. Catal. B*, **17**, 347 (1998).
19. S. Zhen, L. Gao, Q.H. Zhang and J.K. Guo, *Chin. J. Catal.*, **22**, 206 (2001).

(*Received*: 5 April 2010; *Accepted*: 2 July 2010) AJC-8849